Received: 24 January 2016 | Revised: 19 June 2017 | Accepted: 12 July 2017

DOI: 10.1002/num.22191

RESEARCH ARTICLE

WILEY

Multiscale discontinuous Petrov–Galerkin method for the multiscale elliptic problems

Fei Song | **Weibing Deng**

Department of Mathematics, Nanjing University, Jiangsu, 210093, P.R. China

Correspondence
Weibing Deng, Department of Mathematics, Nanjing University, Jiangsu, 210093, P.R. China.
Email: wbdeng@nju.edu.cn

Present address
Fei Song, College of Science, Nanjing Forestry University, Jiangsu, 210037, P.R. China

Funding information
The work of F. S. was partially supported by the University Postgraduate Research and Innovation Project of Jiangsu Province 2014 under Grant KYZZ_0021. The work of W. D. was partially supported by the NSF of China Grant 10971096 and the Project Funded by the Priority Academic Program Development of Jiangsu Higher Education Institutions.

In this article, we present a new multiscale discontinuous Petrov–Galerkin method (MsDPGM) for multiscale elliptic problems. This method utilizes the classical oversampling multiscale basis in the framework of a Petrov–Galerkin version of the discontinuous Galerkin method, allowing us to better cope with multiscale features in the solution. MsDPGM takes advantage of the multiscale Petrov–Galerkin method (MsPGM) and the discontinuous Galerkin method (DGM). It can eliminate the resonance error completely and decrease the computational costs of assembling the stiffness matrix, thus, allowing for more efficient solution algorithms. On the basis of a new H^2 norm error estimate between the multiscale solution and the homogenized solution with the first-order corrector, we give a detailed convergence analysis of the MsDPGM under the assumption of periodic oscillating coefficients. We also investigate a multiscale discontinuous Galerkin method (MsDGM) whose bilinear form is the same as that of the DGM but the approximation space is constructed from the classical oversampling multiscale basis functions. This method has not been analyzed theoretically or numerically in the literature yet. Numerical experiments are carried out on the multiscale elliptic problems with periodic and randomly generated log-normal coefficients. Their results demonstrate the efficiency of the proposed method.

KEYWORDS
error estimate, multiscale discontinuous Petrov–Galerkin method, multiscale problems

1 | INTRODUCTION

This article considers the numerical approximation of second-order elliptic problems with heterogeneous and highly oscillating coefficients. These problems arise in many applications such as flows in porous media or composite materials. The numerical simulation of such problems in heterogeneous media poses significant mathematical and computational challenges. Standard numerical methods such as the finite element method (FEM) or the finite volume method usually require a very fine mesh size. This necessitates a tremendous amount of computer memory and CPU time. In the past few decades, a number of more efficient multiscale numerical methods have been proposed; see, for example, the multiscale finite element method (MsFEM) [1–3], heterogeneous multiscale method (HMM) [4–6], upscaling or numerical homogenization method [7–10], variational multiscale method (or the residual-free bubble method) [11–15], wavelet homogenization techniques [16, 17], and multigrid numerical homogenization techniques [18, 19]. Most of them are presented on meshes that are coarser than the scale of oscillations. The small-scale effect on the coarse scale is either captured by localized multiscale basis functions or modeled into the coarse scale equations with prescribed analytical forms.

In this article, we use the MsFEM framework and propose a new method. The two main ingredients of MsFEM are the global formulation of the method such as various FEMs and the construction of basis functions. The key of MsFEM is to construct a multiscale basis from the local solutions of the elliptic operator for finite element formulation. There have been many extensions and applications of the method in the past fifteen years (cf. [20–31]). We refer the reader to the book [32] for more discussions on the theory and applications of MsFEMs.

It is shown that the oversampling MsFEM is a nonconforming FEM, where the numerical solution has certain continuity across the inner-element boundaries, and its basis functions are discontinuous at the inner-element boundaries (see [1, 2]). Note that DG methods do not require any continuity, which inspires the natural use of the DGM as the global formulation coupled with the oversampling multiscale bases (see [32]). DG methods for elliptic boundary value problems have been studied since the late 1970s, and it is now an active research area (see [33–35]). Examples of the DG methods include the local discontinuous Galerkin (LDG) method [36–38], and the interior penalty discontinuous Galerkin (IPDG) methods [34, 35, 39–43]. In this article, we are concerned with the IPDG method, still named DGM. DG methods permit good local conservation properties of the state variable and also offer the use of very general meshes due to the lack of interelement continuity requirement, for example, meshes that contain several different types of elements or hanging nodes. These features are crucial in many multiscale applications (see [44, 45]).

In the past 10 years, several multiscale methods related to DG methods have been introduced. For instance, a multiscale model reduction technique in the framework of the DGM for use in high–contrast problems, named Generalized Multiscale Finite Element Method, was presented in [46]. The use of special multiscale basis functions of the DG approximation space to capture the singularity of the solutions was discussed in [47–49]. The variational multiscale methods based on the DGM for use in elliptic multiscale problems without any assumption on scale separation or periodicity were proposed in [50, 51]. HMMs based on DGM for homogenization or advection–diffusion problems were presented in [52, 53]. However, to our knowledge, the multiscale discontinuous Galerkin method (MsDGM), which couples the classical oversampling multiscale basis with the discontinuous Galerkin method, has not been studied in detail for error analysis. There is also no numerical testing in the literature. To complete this task, in this article, we provide the formulation and the corresponding error estimate of MsDGM. Our numerical experiments show that MsDGM takes advantages of MsFEM and DGM and thus can eliminate the resonance error and obtain more accurate results than the classical MsFEM.

Further, we noticed that the Petrov–Galerkin (PG) formulation of the multiscale method can decrease the computational costs of assembling the stiffness matrix, leading to more efficient algorithms.

Moreover, it has been found that the MsPGM can eliminate the resonance error using the oversampling technique [2] and the conforming piecewise linear functions as test functions [3, 30]. Therefore, in this article, we try to use the discontinuous oversampling multiscale space in the framework of PG method, which couples both DGM and MsPGM. The proposed method is called the multiscale discontinuous Petrov–Galerkin method (MsDPGM), which has two key issues to consider. The first issue is how to define its bilinear form and prove its coercivity, which requires the transfer operator between the approximation space and the test function space. We emphasize that, compared to MsDGM, the bilinear form of MsDPGM is not just choosing the discontinuous piecewise linear function space as test function space. A finer choice of the terms of the bilinear form should be made. The second issue is error estimate. We give a new H^2 norm error estimate between the multiscale solution and the homogenized solution with the first-order corrector. This error estimate plays an important role in the latter convergence analysis. MsDPGM takes advantage of both MsPGM and DGM and is expected to approximate the multiscale solution better than standard MsPGM.

The proposed method is related to a combined finite element and oversampling multiscale Petrov–Galerkin method (FE-OMsPGM) [45], which utilizes the traditional FEM directly on a fine mesh of the problematic part of the domain and use the OMsPGM on a coarse mesh of the other part. The transmission condition across the FE-OMsPGM interface is treated by the penalty technique of DGM. In [45], the transmission condition is handled by penalizing the jumps from linear function values as well as the fluxes of the finite element solution on the fine mesh to those of the oversampling multiscale solution on the coarse mesh. Compared to [45], in this article, we develop and analyze MsDPGM for multiscale elliptic problems, using the PG formulation based on the discontinuous multiscale approximation space. The jump terms across each interelement are dealt with using a penalty technique. The penalty term of linear function values is taken as that of the FE-OMsPGM while penalizing the fluxes is not needed.

Although the error analysis is done assuming periodic oscillating coefficients, our method is not restricted to the periodic case. The numerical results show that the introduced MsDPGM is very efficient for randomly generated coefficients. Recently, the multiscale methods on localization of the elliptic multiscale problems with highly varying (non-periodic) coefficients are studied in some papers. For instance, the new variational multiscale method is presented in [54]; a new oversampling strategy for the MsFEM is presented in [55]. In our future work, more extensions and developments of our method with the new oversampling strategy will be given.

The outline of this article is as follows. In Section 2, we present the model problem and recall the DG variational formulation of the model problem in the broken Sobolev spaces. Section 3 is devoted to deriving the MsDPGM. It includes the introduction of discontinuous oversampling multiscale approximation space and the derivation of the formulations of MsDGM and MsDPGM. In Section 4, we review the homogenization results and give some preliminaries for the error analysis. In Section 5, we present the main results of our method. It includes the stability and *a priori* error estimate. In Section 6, we first give several numerical examples with periodic coefficients to demonstrate the accuracy of the method. Then we do the experiment to study how the size of oversampling elements affects the errors. Finally, we apply our method to multiscale problems on the L–shaped domain to demonstrate the efficiency of the method. Conclusions are given in the last section.

2 | MODEL PROBLEM AND DG VARIATIONAL FORMULATION

In this section, we introduce the multiscale model problem and give the DG variational formulation of the model problem. First, we state some notation and conventions. Throughout this article, the Einstein summation convention is used: summation is taken over repeated indices. Standard notation

on Lebesgue and Sobolev spaces is employed. Subsequently $C, C_0, C_1, C_2, \cdots$ denote generic constants, which are independent of ε, h, unless otherwise stated. We also use the shorthand notation $A \lesssim B$ and $B \lesssim A$ for the inequality $A \leq CB$ and $B \leq CA$. We write $A \eqsim B$ for $A \lesssim B$ and $B \lesssim A$.

2.1 | Model problem

Let $\Omega \subset \mathbf{R}^n$, $n = 2, 3$, be a bounded polyhedral domain. Consider the following multiscale elliptic problem:

$$\begin{cases} -\nabla \cdot (\mathbf{a}^\varepsilon(x)\nabla u_\varepsilon(x)) = f(x) & \text{in } \Omega, \\ u_\varepsilon(x) = 0 & \text{on } \partial\Omega, \end{cases} \tag{2.1}$$

where $\varepsilon \ll 1$ is a parameter that represents the small scale in the physical problem, $f \in L^2(\Omega)$, and $\mathbf{a}^\varepsilon(x) = (a_{ij}^\varepsilon(x))$ is a symmetric, positive definite matrix:

$$\lambda|\xi|^2 \leq a_{ij}^\varepsilon(x)\xi_i\xi_j \leq \Lambda|\xi|^2 \quad \forall \xi \in \mathbf{R}^n, x \in \overline{\Omega} \tag{2.2}$$

for some positive constants λ and Λ.

2.2 | DG variational formulation

In this subsection, we derive the DG variational formulation of the model problem in the broken Sobolev spaces. Let $\mathcal{T}_h$ be a quasiuniform triangulation of the domain Ω. We define h_K as $\operatorname{diam}(K)$ and denote by $h = \max_{K\in\mathcal{T}_h} h_K$.

We introduce the broken Sobolev spaces for any real number s,

$$H^s(\mathcal{T}_h) = \left\{ v \in L^2(\Omega) : \forall K \in \mathcal{T}_h, v|_K \in H^s(K) \right\},$$

equipped with the broken Sobolev norm:

$$|||v|||_{H^s(\mathcal{T}_h)} = \left(\sum_{K\in\mathcal{T}_h} \|v\|_{H^s(K)}^2 \right)^{1/2}.$$

Denote by Γ_h the set of interior edges/faces of the $\mathcal{T}_h$. With each edge/face e, we associate a unit normal vector $\mathbf{n}$. If e is on the boundary $\partial\Omega$, then $\mathbf{n}$ is taken to be the unit outward vector normal to $\partial\Omega$.

If $v \in H^1(\mathcal{T}_h)$, the trace of v along any side of one element K is well defined. If two elements K_1^e and K_2^e are neighbors and share a common side e, there are two traces of v along e. We define the average and jump for v. Assume that the normal vector $\mathbf{n}$ is oriented from K_1^e to K_2^e:

$$\{v\} := \frac{v|_{K_1^e} + v|_{K_2^e}}{2}, \qquad [v] := v|_{K_1^e} - v|_{K_2^e} \qquad \forall e = \partial K_1^e \cap \partial K_2^e. \tag{2.3}$$

We extend the definition of jump and average to sides that belong to the boundary $\partial\Omega$:

$$\{v\} = [v] = v|_{K_1^e} \qquad \forall e = \partial K_1^e \cap \partial\Omega.$$

In the following, assume that $s=2$. Multiplying (2.1) by any $v \in H^s(\mathcal{T}_h)$, integrating on each element K, and using integration by parts, we obtain

$$\int_K \mathbf{a}^\varepsilon \nabla u_\varepsilon \cdot \nabla v \, \mathrm{d}x - \int_{\partial K} \mathbf{a}^\varepsilon \nabla u_\varepsilon \cdot \mathbf{n}_K v \, \mathrm{d}s = \int_K fv.$$

Recall that $\mathbf{n}_K$ is the outward normal to K. Summing over all elements and switching to the normal vectors $\mathbf{n}$ yield

$$\sum_{K\in\mathcal{T}_h} \int_{\partial K} \mathbf{a}^\varepsilon \nabla u_\varepsilon \cdot \mathbf{n}_K v \, \mathrm{d}s = \sum_{e\in\Gamma_h\cup\partial\Omega} \int_e [\mathbf{a}^\varepsilon \nabla u_\varepsilon \cdot \mathbf{n} v] \, \mathrm{d}s.$$

From the regularity of the solution u_ε, it follows that

$$\sum_{K\in\mathcal{T}_h} \int_K \mathbf{a}^\varepsilon \nabla u_\varepsilon \cdot \nabla v \, \mathrm{d}x - \sum_{e\in\Gamma_h\cup\partial\Omega} \int_e \{\mathbf{a}^\varepsilon \nabla u_\varepsilon \cdot \mathbf{n}\}[v] \mathrm{d}s = \int_\Omega fv,$$

where we have used the formula $[vw] = \{v\}[w] + [v]\{w\}$ and the fact that $[\mathbf{a}^\varepsilon \nabla u_\varepsilon \cdot \mathbf{n}] = 0$.

We now define the DG bilinear form $a(\cdot,\cdot): H^s(\mathcal{T}_h) \times H^s(\mathcal{T}_h) \to \mathbf{R}$:

$$\begin{aligned} a(u,v) := &\sum_{K\in\mathcal{T}_h} \int_K \mathbf{a}^\varepsilon \nabla u \cdot \nabla v \, \mathrm{d}x - \sum_{e\in\Gamma_h\cup\partial\Omega} \int_e \{\mathbf{a}^\varepsilon \nabla u \cdot \mathbf{n}\}[v] \mathrm{d}s \\ &+ \beta \sum_{e\in\Gamma_h\cup\partial\Omega} \int_e [u]\{\mathbf{a}^\varepsilon \nabla v \cdot \mathbf{n}\} \mathrm{d}s + \sum_{e\in\Gamma_h\cup\partial\Omega} \frac{\gamma_0}{\rho} \int_e [u][v] \mathrm{d}s, \end{aligned}$$

where β is a real number such as $-1, 0, 1$, γ_0 is called penalty parameter, and $\rho > 0$ will be specified later.

The general DG variational formulation of the problem (2.1) is as follows: Find $u_\varepsilon \in H^s(\mathcal{T}_h)$ such that

$$a(u_\varepsilon, v) = (f, v) \qquad \forall v \in H^s(\mathcal{T}_h). \tag{2.4}$$

Remark 2.1 It is easy to check that if the solution u_ε of problem (2.1) belongs to $H^2(\Omega)$, then u_ε satisfies the variational formulation (2.4). Conversely, if $u_\varepsilon \in H^1(\Omega) \cap H^s(\mathcal{T}_h)$ satisfies (2.4), then u_ε is the solution of problem (2.1).

3 | MULTISCALE DISCONTINUOUS PETROV-GALERKIN METHOD

This section is devoted to the formulations of multiscale discontinuous methods for solving (2.1). In Subsection 3.1, we introduce the oversampling multiscale approximation space defined on the triangulation $\mathcal{T}_h$. The formulations of the MsDG and MsDPG methods are presented in Subsection 3.2.

3.1 | Oversampling multiscale approximation space

This subsection introduces the oversampling multiscale approximation space defined on the triangulation $\mathcal{T}_h$ (cf. [2, 32, 56]). Here, we only consider the case where $n=2$. For any $K \in \mathcal{T}_h$ with nodes $\left\{x_i^K\right\}_{i=1}^3$,

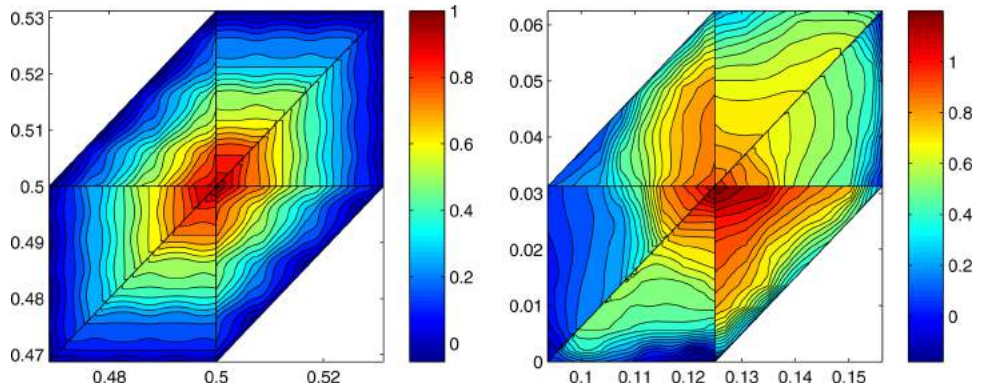

FIGURE 1 Example of oversampling basis functions. Left: basis function for periodic media. Right: basis function for random media [Color figure can be viewed at wileyonlinelibrary.com]

let $\left\{\varphi_i^K\right\}_{i=1}^3$ be the basis of $P_1(K)$ satisfying $\varphi_i^K(x_j^K) = \delta_{ij}$, where δ_{ij} stands for the Kroneckers symbol. For any $K \in \mathcal{T}_h$, we denote by $S = S(K)$ a macroelement which contains K and $d_K = \text{dist}(\partial S, K)$. We assume that $d_K \geq \delta_0 h_K$ for some positive constant δ_0 independent of h_K. The minimum angle of $S(K)$ is bounded from below by some positive constant θ_0 independent of h_K. In our later numerical experiments, for any element $K \in \mathcal{T}_h$ we put its macroelement $S(K)$ in such a way that their barycenters are coinciding and their corresponding edges are parallel. See Figure 2 for an illustration.

Let $\psi_i^S, i = 1, 2, 3$, with $\psi_i^S \in H^1(S)$, be the solution of the problem:

$$-\nabla \cdot (\mathbf{a}^\varepsilon \nabla \psi_i^S) = 0 \qquad \text{in } S, \qquad \psi_i^S|_{\partial S} = \varphi_i^S. \tag{3.1}$$

Here $\left\{\varphi_i^S\right\}_{i=1}^3$ is the nodal basis of $P_1(S)$ such that $\varphi_i^S(x_j^S) = \delta_{ij}, i, j = 1, 2, 3$.

The oversampling multiscale basis functions on K are defined by

$$\overline{\psi_i}^K = \sum_{j=1}^3 c_{ij}^K \psi_j^S|_K \qquad \text{in } K, \tag{3.2}$$

with the constants so chosen that

$$\varphi_i^K = \sum_{j=1}^3 c_{ij}^K \varphi_j^S|_K \qquad \text{in } K. \tag{3.3}$$

The existence of the constants c_{ij}^K is guaranteed because $\left\{\varphi_j^S\right\}_{j=1}^3$ also forms the basis of $P_1(K)$. To illustrate the basis functions, we depict two examples of them in Figure 1 (cf. [45]).

Let $\text{OMS}(K) = \text{span}\left\{\overline{\psi_i}^K\right\}_{i=1}^3$ be the set of space functions on K. Define the projection $\Pi_K : \text{OMS}(K) \to P_1(K)$ as follows:

$$\Pi_K \psi = c_i \varphi_i^K \qquad \text{if} \qquad \psi = c_i \overline{\psi}_i^K \in \text{OMS}(K).$$

Further, we introduce the discontinuous piecewise "OMS" approximation space and the discontinuous piecewise linear space:

$$V_{h,dc}^{ms} = \left\{\psi_h \in L^2(\Omega) : \psi_h|_K \in \text{OMS}(K) \qquad \forall K \in \mathcal{T}_h\right\},$$

$$V_{h,dc} = \left\{ v_h \in L^2(\Omega) : v_h|_K \in P_1(K) \qquad \forall K \in \mathcal{T}_h \right\}.$$

Here we use the abbreviated indexes "ms," "dc" for multiscale, discontinuous, respectively.

3.2 | Formulation of the MsDGM/MsDPGM

Using the DG variational formulation (2.4) and the discontinuous piecewise "OMS" approximation space, we are now ready to define the MsDG method: Find $\tilde{u}_h \in V_{h,dc}^{ms}$ such that

$$a(\tilde{u}_h, v_h) = (f, v_h) \qquad \forall v_h \in V_{h,dc}^{ms}. \tag{3.4}$$

To define the discrete bilinear form for MsDPGM, we need the transfer operator $\Pi_h : V_{h,dc}^{ms} \to V_{h,dc}$ as following:

$$\Pi_h \psi_h|_K = \Pi_K \psi_h \quad \text{for any } K \in \mathcal{T}_h, \psi_h \in V_{h,dc}^{ms}.$$

Remark 3.1 In general, the trial and test functions of PGM are not in the same space. For example, here we might use $V_{h,dc}^{ms}$ and $V_{h,dc}$ as the trial function and test function spaces respectively. However, it may result in a difficulty to prove the inf-sup condition of the corresponding bilinear form. Hence, in this article, we introduce the transfer operator Π_h to connect the two spaces and use it in the bilinear form which causes a simple way to establish the stability of the MsDPGM. The idea of connecting the trial function and test function spaces in the Petrov-Galerkin method through an operator was introduced in [57] (see also [58]).

The discrete bilinear form of MsDPGM on $V_{h,dc}^{ms} \times V_{h,dc}^{ms}$ is defined as:

$$\begin{aligned} a_h(u_h, v_h) :=& \sum_{K \in \mathcal{T}_h} \int_K \mathbf{a}^\varepsilon \nabla u_h \cdot \nabla \Pi_h v_h \, \mathrm{d}x \\ &- \sum_{e \in \Gamma_h \cup \partial\Omega} \int_e \{\mathbf{a}^\varepsilon \nabla u_h \cdot \mathbf{n}\} [\Pi_h v_h] \mathrm{d}s \\ &+ \beta \sum_{e \in \Gamma_h \cup \partial\Omega} \int_e [\Pi_h u_h] \{\mathbf{a}^\varepsilon \nabla v_h \cdot \mathbf{n}\} \mathrm{d}s \\ &+ J_0(u_h, v_h), \\ J_0(u_h, v_h) :=& \sum_{e \in \Gamma_h \cup \partial\Omega} \frac{\gamma_0}{\rho} \int_e [\Pi_h u_h][\Pi_h v_h] \mathrm{d}s, \end{aligned}$$

where β is a real number such as $-1, 0, 1$, γ_0 is the penalty parameter, and ρ will be specified later.

Remark 3.2 It is well known that DG methods utilize discontinuous piecewise polynomial functions and numerical fluxes, which implies that the weak formulation subject to discretization must include jump terms across interfaces and that some penalty terms must be added to control the jump terms. Therefore, the methods require the restriction on the penalty parameter to ensure stability and convergence in some sense. In fact, the optional convergence is related with the penalty parameter (see [59]). In this article, the

MsDPGM takes advantage of the penalty technique, which involves the selection of the penalty parameter. In the theoretical analysis, the penalty parameter γ_0 is constrained by a large constant from below to ensure the coercivity of a_h. However, in practice, the penalty parameter is chosen through our experience. In following numerical tests, we try a different choice of the penalty parameter to study its affection on the error.

Remark 3.3 The parameter ρ is chosen as ε in our later error analysis, which means the theory requires an over-penalization in respect to h as in general, we assume that $\varepsilon \ll h$. However, for the random coefficient case, there is no explicit ε in the multiscale problem. In this case, we choose ρ as h.

Then, our MsDPG method is: Find $u_h \in V_{h,dc}^{ms}$ such that

$$a_h(u_h, v_h) = (f, \Pi_h v_h) \qquad \forall v_h \in V_{h,dc}^{ms}. \tag{3.5}$$

Remark 3.4 The design of the last two terms in a_h is tricky. As a matter of fact, we have tried numerically different possibilities of using Π_h (or not before each u_h or v_h) before we found that the current form of a_h is the best one and, most importantly, the corresponding MsDPGM can be analyzed theoretically. Indeed, our MsDPGM is a certain pseudo Petrov-Galerkin formulation of the method that the test function space is formally the same as the solution space. However, some terms involve a projection of the multiscale test function into a piecewise linear function space.

We let the discrete norm for MsDPGM on $V_{h,dc}^{ms}$ be

$$\begin{aligned}\|v_h\|_{h,\Omega} := \Bigg(&\sum_{K\in\mathcal{T}_h} \int_K \mathbf{a}^\varepsilon \nabla v_h \cdot \nabla v_h \,\mathrm{d}x + \sum_{e\in\Gamma_h\cup\partial\Omega} \frac{\rho}{\gamma_0} \int_e \{\mathbf{a}^\varepsilon \nabla v_h \cdot \mathbf{n}\}^2 \mathrm{d}s \\ &+ \sum_{e\in\Gamma_h\cup\partial\Omega} \frac{\gamma_0}{\rho} \int_e [\Pi_h v_h]^2 \,\mathrm{d}s \Bigg)^{1/2}.\end{aligned}$$

Noting that the operator Π_h is not defined for the exact solution u_ε, we introduce the following function to measure the error of the discrete solution:

$$\begin{aligned}E(v, v_h) := \Bigg(&\sum_{K\in\mathcal{T}_h} \|(\mathbf{a}^\varepsilon)^{1/2} \nabla (v - v_h)\|_{L^2(K)}^2 \\ &+ \sum_{e\in\Gamma_h\cup\partial\Omega} \frac{\rho}{\gamma_0} \| \{\mathbf{a}^\varepsilon \nabla (v - v_h) \cdot \mathbf{n}\} \|_{L^2(e)}^2 \\ &+ \sum_{e\in\Gamma_h\cup\partial\Omega} \frac{\gamma_0}{\rho} \|[v - \Pi_h v_h]\|_{L^2(e)}^2 \Bigg)^{1/2} \qquad \forall v \in H^2(\Omega), v_h \in V_{h,dc}^{ms}.\end{aligned} \tag{3.6}$$

From the triangle inequality, it is clear that, for any $v \in H^2(\Omega), v_h, w_h \in V_{h,dc}^{ms}$,

$$E(v, v_h) \lesssim E(v, w_h) + \|w_h - v_h\|_{h,\Omega}. \tag{3.7}$$

4 | HOMOGENIZATION RESULTS AND PRELIMINARIES

In this section, we first review the results of classical homogenization theory and give an important H^2 norm error estimate between the multiscale solution and the homogenized solution with the first order corrector. Then, we recall some preliminaries for our later analysis.

4.1 | The homogenization results

Hereafter, we assume that $\mathbf{a}^\varepsilon(x)$ has the form $\mathbf{a}(x/\varepsilon)$ and $a_{ij}(y)$ are sufficiently smooth periodic functions in y with respect to a unit cube Y. For our analysis, it is sufficient to assume that $a_{ij}(y) \in W^{2,p}(Y)$ with $p > n$.

For convenience, we take

$$u_1 = u_0 + \varepsilon \chi^j(x/\varepsilon)\frac{\partial u_0}{\partial x_j},$$

where u_0 is the homogenized solution, χ^j is the periodic solution of the following cell problem (cf. [60, 61]):

$$-\nabla_y \cdot (\mathbf{a}(y)\nabla_y \chi^j(y)) = \nabla_y \cdot (\mathbf{a}(y)\mathbf{e}_j), \quad j = 1, \cdots, n \tag{4.1}$$

with zero mean, that is, $\int_Y \chi^j dy = 0$, and $\mathbf{e}_j$ is the unit vector in the jth direction.

The following theorem gives the H^2 semi-norm estimate of the error $u_\varepsilon - u_1$, which plays a pivotal role in the error analysis. We arrange the proof in the Appendix A.

Theorem 4.1 *Assume that $u_0 \in H^3(\Omega)$. Then, the following estimate is valid:*

$$|u_\varepsilon - u_1|_{H^2(\Omega)} \lesssim |u_0|_{H^2(\Omega)} + \frac{1}{\sqrt{\varepsilon}}|u_0|_{W^{1,\infty}(\Omega)} + \varepsilon |u_0|_{H^3(\Omega)}. \tag{4.2}$$

4.2 | Preliminaries

In this subsection, we give some preliminaries for subsequent analysis. We first recall the definition of $\psi_i^S, i = 1, 2, 3$ (see [3.1]). By the asymptotic expansion (cf. [1, 30]), we know that

$$\psi_i^S = \varphi_i^S + \varepsilon \chi^j(x/\varepsilon)\frac{\partial \varphi_i^S}{\partial x_j} + \varepsilon \eta^j(x)\frac{\partial \varphi_i^S}{\partial x_j}, \tag{4.3}$$

with η^j being the solution of

$$-\nabla \cdot (\mathbf{a}^\varepsilon \nabla \eta^j) = 0 \qquad \text{in } S, \qquad \eta^j|_{\partial S} = -\chi^j(x/\varepsilon). \tag{4.4}$$

Substituting (4.3) to (3.2), we see that $\overline{\psi_i}^K$ can be expanded as follows:

$$\overline{\psi_i}^K = \varphi_i^K + \varepsilon \chi^j(x/\varepsilon)\frac{\partial \varphi_i^K}{\partial x_j} + \varepsilon \eta^j(x)\frac{\partial \varphi_i^K}{\partial x_j}. \tag{4.5}$$

Recall that $d_K = \text{dist}(\partial S, K)$, which satisfies: $d_K \geq \delta_0 h_K$. Denote by $d = \min_{K \in \mathcal{T}_h} d_K$.

Remark 4.1 It has been shown in [2, 30] that the distance d_K is determined by the thickness of the boundary layer of η^j. Numerically, it has been observed that the boundary layer of η^j is about $O(\varepsilon)$ thick (see [2]). It was also observed that $d_K = h_K (> \varepsilon)$ is usually sufficient for eliminating the boundary layer effect. Therefore, in our numerical tests we choose h_K as the oversampling size in this article. To study how the size of oversampling elements affects the errors, in Section 6 we include a numerical test which uses a series of d_K with different δ_0 to compare the corresponding errors.

By the Maximum Principle we have

$$\|\eta^j\|_{L^\infty(S)} \leq |\chi^j|_{L^\infty(S)} \lesssim 1, \tag{4.6}$$

which together with the interior gradient estimate (see [44, Lemma 3.6] or [1, Proposition C.1]) implies that

$$\|\nabla \eta^j\|_{L^\infty(K)} \lesssim \frac{1}{d_K}. \tag{4.7}$$

Next, we give a trace inequality which will be used in this article frequently (see [62, Theorem 1.6.6], [63]).

Lemma 4.1 *Let K be an element of the triangulation $\mathcal{T}_h$. Then, for any $v \in H^1(K)$, we have*

$$\|v\|_{L^2(\partial K)} \leq C \left(diam(K)^{-1/2} \|v\|_{L^2(K)} + \|v\|_{L^2(K)}^{1/2} \|\nabla v\|_{L^2(K)}^{1/2} \right). \tag{4.8}$$

The following lemma gives some approximation properties of the space OMS(K) (cf. [44, Lemma 4.1]).

Lemma 4.2 *Take $\phi_h^K = \sum_{x_i^K \text{ node of } K} u_0(x_i^K) \overline{\psi}_i^K(x), \quad \forall K \in \mathcal{T}_h$. Then, the following estimates hold:*

$$|u_1 - \phi_h^K|_{H^1(K)} \lesssim h_K |u_0|_{H^2(K)} + \varepsilon h_K^{n/2} d_K^{-1} |u_0|_{W^{1,\infty}(K)}, \tag{4.9}$$

$$\|u_1 - \phi_h^K\|_{L^2(K)} \lesssim h_K^2 |u_0|_{H^2(K)} + \varepsilon h_K^{n/2} |u_0|_{W^{1,\infty}(K)}, \tag{4.10}$$

$$|u_1 - \phi_h^K|_{H^2(K)} \lesssim \varepsilon^{-1} h_K |u_0|_{H^2(K)} + h_K^{n/2} d_K^{-1} |u_0|_{W^{1,\infty}(K)} + \varepsilon |u_0|_{H^3(K)}. \tag{4.11}$$

Moreover, we recall the stability estimate for Π_K, which will be used in our later analysis (cf. Lemma 3.2 in [45]).

Lemma 4.3 *There exist positive constants γ, α_1, and α_2 which are independent of h and ε such that if $\varepsilon / h_K \leq \gamma$ for all $K \in \mathcal{T}_h$, then the following estimates are valid for any $v_h \in OMS(K)$,*

$$\|\nabla v_h\|_{L^2(K)} \eqsim \|\nabla \Pi_K v_h\|_{L^2(K)}, \tag{4.12}$$

$$\alpha_2 \|\nabla v_h\|_{L^2(K)}^2 \leq \left| \int_K \mathbf{a}^\varepsilon \nabla v_h \cdot \nabla \Pi_K v_h \, dx \right| \leq \alpha_1 \|\nabla v_h\|_{L^2(K)}^2. \tag{4.13}$$

The following lemma gives an inverse estimate for the function in space $\mathrm{OMS}(K)$ [44, Lemma 5.2].

Lemma 4.4 *Under the assumptions of Lemma 4.3, and assuming $\varepsilon \lesssim h_K \lesssim d_K$, we have*

$$|v_h|_{H^2(K)} \lesssim \frac{1}{\varepsilon}\|\nabla v_h\|_{L^2(K)} \quad \forall v_h \in OMS(K). \tag{4.14}$$

5 | MAIN RESULTS

In this section, we only carry out the convergence analysis of MsDPGM. For MsDGM, similar results can be obtained by the same argument and are arranged in the Appendix B for the convenience of the reader. For MsDPGM, we first show the stability of the bilinear form guaranteeing the existence and uniqueness of the solution and then prove the error estimate with $\beta = -1, \rho = \varepsilon$. We omit other cases such as $\beta = 0, 1$ as the analysis is similar.

5.1 | Existence and uniqueness of the solution of MsDPGM

We start by establishing the stability of the bilinear form of MsDPGM.

Theorem 5.1 *We have*

$$|a_h(u_h, v_h)| \le C\|u_h\|_{h,\Omega}\|v_h\|_{h,\Omega} \qquad \forall u_h, v_h \in V_{h,dc}^{ms}. \tag{5.1}$$

Further, let the assumptions of Lemma 4.4 be fulfilled and γ_0 be large enough. Then,

$$a_h(v_h, v_h) \ge \kappa\|v_h\|_{h,\Omega}^2 \qquad \forall v_h \in V_{h,dc}^{ms}, \tag{5.2}$$

where $\kappa > 0$ is a constant independent of h, ε, γ_0

Proof From the definition of the norms, the Cauchy-Schwarz inequality, and Lemma 4.3, (5.1) follows immediately.

Next, we prove (5.2). From (4.13), we get

$$\begin{aligned} a_h(v_h, v_h) \ge C \sum_{K\in\mathcal{T}_h} \|(\mathbf{a}^\varepsilon)^{1/2}\nabla v_h\|_{L^2(K)}^2 - 2\sum_{e\in\Gamma_h\cup\partial\Omega}\int_e \{\mathbf{a}^\varepsilon\nabla v_h\cdot\mathbf{n}\}[\Pi_h v_h]\mathrm{d}s \\ + \sum_{e\in\Gamma_h\cup\partial\Omega}\frac{\gamma_0}{\varepsilon}\|[\Pi_h v_h]\|_{L^2(e)}^2. \end{aligned}$$

It is easy to see:

$$\begin{aligned} &2\sum_{e\in\Gamma_h\cup\partial\Omega}\int_e \{\mathbf{a}^\varepsilon\nabla v_h\cdot\mathbf{n}\}[\Pi_h v_h]\mathrm{d}s \\ &\le 2\sum_{e\in\Gamma_h\cup\partial\Omega}\|\{\mathbf{a}^\varepsilon\nabla v_h\cdot\mathbf{n}\}\|_{L^2(e)}\|[\Pi_h v_h]\|_{L^2(e)} \\ &\le \sum_{e\in\Gamma_h\cup\partial\Omega}\frac{\gamma_0}{2\varepsilon}\|[\Pi_h v_h]\|_{L^2(e)}^2 + \sum_{e\in\Gamma_h\cup\partial\Omega}\frac{2\varepsilon}{\gamma_0}\|\{\mathbf{a}^\varepsilon\nabla v_h\cdot\mathbf{n}\}\|_{L^2(e)}^2. \end{aligned}$$

Hence, we obtain

$$\begin{aligned} a_h(v_h, v_h) &\geq C \sum_{K\in\mathcal{T}_h} \|(\mathbf{a}^\varepsilon)^{1/2}\nabla v_h\|^2_{L^2(K)} - \frac{1}{2}\sum_{e\in\Gamma_h\cup\partial\Omega} \frac{\gamma_0}{\varepsilon}\|[\Pi_h v_h]\|^2_{L^2(e)} \\ &\quad - 2\sum_{e\in\Gamma_h\cup\partial\Omega} \frac{\varepsilon}{\gamma_0}\| \{\mathbf{a}^\varepsilon\nabla v_h\cdot\mathbf{n}\} \|^2_{L^2(e)} + \sum_{e\in\Gamma_h\cup\partial\Omega} \frac{\gamma_0}{\varepsilon}\|[\Pi_h v_h]\|^2_{L^2(e)} \\ &= C \sum_{K\in\mathcal{T}_h} \|(\mathbf{a}^\varepsilon)^{1/2}\nabla v_h\|^2_{L^2(K)} + \frac{1}{2}\sum_{e\in\Gamma_h\cup\partial\Omega} \frac{\gamma_0}{\varepsilon}\|[\Pi_h v_h]\|^2_{L^2(e)} \\ &\quad + \frac{1}{2}\sum_{e\in\Gamma_h\cup\partial\Omega} \frac{\varepsilon}{\gamma_0}\| \{\mathbf{a}^\varepsilon\nabla v_h\cdot\mathbf{n}\} \|^2_{L^2(e)} - \frac{5}{2}\sum_{e\in\Gamma_h\cup\partial\Omega} \frac{\varepsilon}{\gamma_0}\| \{\mathbf{a}^\varepsilon\nabla v_h\cdot\mathbf{n}\} \|^2_{L^2(e)}. \end{aligned} \tag{5.3}$$

By Lemmas 4.1, 4.4 and $\varepsilon \lesssim h$, we have

$$\frac{\varepsilon}{\gamma_0}\| \{\mathbf{a}^\varepsilon\nabla v_h\cdot\mathbf{n}\} \|^2_{L^2(e)} \leq \frac{C_1}{\gamma_0}\|(\mathbf{a}^\varepsilon)^{1/2}\nabla v_h\|^2_{L^2(K)}. \tag{5.4}$$

Therefore, from (5.3) and (5.4), we get

$$\begin{aligned} a_h(v_h, v_h) &\geq \left(C - \frac{5C_1}{2\gamma_0}\right)\sum_{K\in\mathcal{T}_h} \|(\mathbf{a}^\varepsilon)^{1/2}\nabla v_h\|^2_{L^2(K)} \\ &\quad + \frac{1}{2}\sum_{e\in\Gamma_h\cup\partial\Omega} \frac{\varepsilon}{\gamma_0}\| \{\mathbf{a}^\varepsilon\nabla v_h\cdot\mathbf{n}\} \|^2_{L^2(e)} \\ &\quad + \frac{1}{2}\sum_{e\in\Gamma_h\cup\partial\Omega} \frac{\gamma_0}{\varepsilon}\|[\Pi_h v_h]\|^2_{L^2(e)}, \end{aligned}$$

where γ_0 is large enough such that $\frac{5C_1}{2\gamma_0} < \frac{C}{2}$. Choosing $\kappa = \min\left(\frac{C}{2}, \frac{1}{2}\right)$ yields (5.2). This completes the proof. ∎

Theorem 5.1 guarantees the existence of a unique solution to our MsDPGM. Now we establish an analog of the Céa lemma written in the following theorem:

Theorem 5.2 *For large enough γ_0, the following inequality holds:*

$$E(u_\varepsilon, u_h) \lesssim \inf_{v_h\in V^{ms}_{h,dc}} E(u_\varepsilon, v_h), \tag{5.5}$$

where the error function E is defined in (3.6).

Proof It is clear that by Theorem 5.1, we have

$$\begin{aligned} \|u_h - v_h\|^2_{h,\Omega} &\lesssim a_h(u_h - v_h, u_h - v_h) \\ &= a_h(u_h, u_h - v_h) - a_h(v_h, u_h - v_h) \\ &= (f, \Pi_h(u_h - v_h)) - a_h(v_h, u_h - v_h). \end{aligned}$$

From (2.4), it follows that

$$(f, \Pi_h(u_h - v_h)) = \sum_{K\in\mathcal{T}_h} \int_K \mathbf{a}^\varepsilon \nabla u_\varepsilon \cdot \nabla \Pi_h(u_h - v_h)\mathrm{d}x - \sum_{e\in\Gamma_h\cup\partial\Omega} \int_e \{\mathbf{a}^\varepsilon \nabla u_\varepsilon \cdot \mathbf{n}\}[\Pi_h(u_h - v_h)]\mathrm{d}s.$$

Then, with $[u_\varepsilon] = 0$ and $[\mathbf{a}^\varepsilon \nabla u_\varepsilon \cdot \mathbf{n}] = 0$, we arrive at

$$\begin{aligned}
&(f, \Pi_h(u_h - v_h)) - a_h(v_h, u_h - v_h)\\
&\quad= \sum_{K\in\mathcal{T}_h} \int_K \mathbf{a}^\varepsilon \nabla(u_\varepsilon - v_h) \cdot \nabla \Pi_h(u_h - v_h)\mathrm{d}x\\
&\qquad- \sum_{e\in\Gamma_h\cup\partial\Omega} \int_e \{\mathbf{a}^\varepsilon \nabla(u_\varepsilon - v_h) \cdot \mathbf{n}\}[\Pi_h(u_h - v_h)]\mathrm{d}s\\
&\qquad+ \sum_{e\in\Gamma_h\cup\partial\Omega} \int_e \{\mathbf{a}^\varepsilon \nabla(u_h - v_h) \cdot \mathbf{n}\}[\Pi_h v_h - u_\varepsilon]\mathrm{d}s\\
&\qquad- \sum_{e\in\Gamma_h\cup\partial\Omega} \frac{\gamma_0}{\varepsilon} \int_e [\Pi_h v_h - u_\varepsilon][\Pi_h(u_h - v_h)]\mathrm{d}s\\
&\quad\lesssim E(u_\varepsilon, v_h)\|u_h - v_h\|_{h,\Omega}.
\end{aligned}$$

Therefore, we obtain

$$\|u_h - v_h\|_{h,\Omega} \lesssim E(u_\varepsilon, v_h),$$

which together with (3.7) yields

$$E(u_\varepsilon, u_h) \lesssim E(u_\varepsilon, v_h) + \|u_h - v_h\|_{h,\Omega} \lesssim E(u_\varepsilon, v_h).$$

The proof is completed. ∎

5.2 | A priori error estimate of MsDPGM

We present the main result of the paper on the error estimate of the MsDPGM.

Theorem 5.3 *Let u_ε be the solution of (2.1), and let u_h be the numerical solution computed using MsDPGM defined by (3.5). Assume that $u_0 \in H^3(\Omega), f \in L^2(\Omega)$, and that $\varepsilon \lesssim h \lesssim d$, and that the penalty parameter γ_0 is large enough. Then there exists a constant γ independent of h and ε such that if $\varepsilon/h_K \le \gamma$ for all $K \in \mathcal{T}_h$, the following error estimate holds:*

$$E(u_\varepsilon, u_h) \lesssim \sqrt{\varepsilon} + \frac{\varepsilon}{d} + h + \frac{h^{3/2}}{\sqrt{\varepsilon}}, \tag{5.6}$$

where $d = min_{K\in\mathcal{T}_h} d_K$.

Proof According to Theorem 5.2, the proof is devoted to estimating the interpolation error. To do this, we define ψ_h by

$$\psi_h|_K = \phi_h^K = \sum_{x_i^K \text{ node of } K} u_0(x_i^K)\overline{\psi}_i^K(x) \quad \forall K \in \mathcal{T}_h. \tag{5.7}$$

Clearly, $\psi_h \in V_{h,dc}^{ms}$. It is easy to see that

$$\Pi_K \phi_h^K = I_h u_0|_K,$$

where $I_h : H^s(\mathcal{T}_h) \to V_{h,dc}$ is the Lagrange interpolation operator. Then, we set v_h as ψ_h. It is shown that in [44],

$$\begin{aligned}&\left(\sum_{K\in\mathcal{T}_h} \|(\mathbf{a}^\varepsilon)^{1/2}\nabla(u_\varepsilon - v_h)\|_{L^2(K)}^2\right)^{1/2}\\ &\quad\lesssim h|u_0|_{H^2(\Omega)} + \sqrt{\varepsilon}|u_0|_{W^{1,\infty}(\Omega)} + \frac{\varepsilon}{d}|u_0|_{W^{1,\infty}(\Omega)}.\end{aligned} \tag{5.8}$$

Next, we estimate the term

$$\sum_{e\in\Gamma_h\cup\partial\Omega} \frac{\varepsilon}{\gamma_0}\| \{\mathbf{a}^\varepsilon\nabla(u_\varepsilon - v_h)\cdot\mathbf{n}\} \|_{L^2(e)}^2 := \mathrm{I}.$$

From (4.8), we have

$$\begin{aligned}\mathrm{I} \lesssim\ & \varepsilon h^{-1}\|\nabla(u_\varepsilon - u_1)\|_{L^2(\Omega)}^2 + \varepsilon h^{-1}\sum_{K\in\mathcal{T}_h}\|\nabla(u_1 - \psi_h)\|_{L^2(K)}^2\\ &+ \varepsilon\|\nabla(u_\varepsilon - u_1)\|_{L^2(\Omega)}^2\|\nabla^2(u_\varepsilon - u_1)\|_{L^2(\Omega)}^2\\ &+ \varepsilon\left(\sum_{K\in\mathcal{T}_h}\|\nabla(u_1 - \psi_h)\|_{L^2(K)}^2\right)^{1/2}\left(\sum_{K\in\mathcal{T}_h}\|\nabla^2(u_1 - \psi_h)\|_{L^2(K)}^2\right)^{1/2}.\end{aligned}$$

Therefore, it follows from Theorem 4.1, Lemma 4.2, and the assumption $\varepsilon \lesssim h \lesssim d$ that,

$$\mathrm{I} \lesssim h^2|u_0|_{H^2(\Omega)}^2 + \varepsilon|u_0|_{W^{1,\infty}(\Omega)}^2 + \varepsilon^4|u_0|_{H^3(\Omega)}^2, \tag{5.9}$$

where we have used $\frac{\varepsilon}{\sqrt{h}} < \sqrt{\varepsilon}$ and the Young's inequality to derive the above inequality.

It remains to consider the term $\sum_{e\in\Gamma_h\cup\partial\Omega}\frac{\gamma_0}{\varepsilon}\|[u_\varepsilon - \Pi_h v_h]\|_{L^2(e)}^2$. Noting that both u_ε and u_0 are continuous functions, we have

$$\begin{aligned}\sum_{e\in\Gamma_h\cup\partial\Omega}\frac{\gamma_0}{\varepsilon}\|[u_\varepsilon - \Pi_h v_h]\|_{L^2(e)}^2 &= \sum_{e\in\Gamma_h\cup\partial\Omega}\frac{\gamma_0}{\varepsilon}\int_e [u_0 - \Pi_h v_h]^2 \mathrm{d}s\\ &\lesssim \sum_{e\in\Gamma_h\cup\partial\Omega}\frac{\gamma_0}{\varepsilon}\int_e (u_0 - \Pi_h\psi_h)^2\,\mathrm{d}s := \mathrm{II}.\end{aligned}$$

Then, by use of Lemma 4.1, we have

$$\begin{aligned}\int_e (u_0 - \Pi_h \psi_h)^2 \mathrm{d}s &= \int_e (u_0 - I_h u_0)^2 \mathrm{d}s \\ &\lesssim h^{-1} \|u_0 - I_h u_0\|^2_{L^2(K)} + \|u_0 - I_h u_0\|_{L^2(K)} \|\nabla(u_0 - I_h u_0)\|_{L^2(K)} \\ &\lesssim h^3 |u_0|^2_{H^2(K)},\end{aligned}$$

which yields

$$\mathrm{II} \lesssim \frac{h^3}{\varepsilon} |u_0|^2_{H^2(\Omega)}. \tag{5.10}$$

Hence, from (5.8-5.10), it follows (5.6) immediately. ∎

6 | NUMERICAL EXPERIMENTS

In this section, we present numerical experiments to confirm the theoretical findings in Section 5. We present the numerical results of MsDPGM (3.5) and those of MsDGM (3.4). To illustrate the accuracy of our methods, we also implement the multiscale Petrov–Galerkin method (MsPGM) and the oversampling multiscale Petrov–Galerkin method (OMsPGM; see [30]). We also show the results of the traditional linear finite element method (FEM) and discontinuous Galerkin method (DGM) on the corresponding coarse grid to get a feeling for the accuracy of the multiscale methods. All numerical experiments are designed to demonstrate that MsDPGM has better performance than the other MsPGMs.

For simplicity, we use in tests the standard triangulation, which is constructed by first dividing the domain Ω into subsquares of equal length h and then connecting the lower-left and the upper-right vertices of each subsquare. For any element $K \in \mathcal{T}_h$ we put its macroelement $S(K)$ in such a way that their barycenters are coinciding and their corresponding edges are parallel. The lengths of the horizontal and vertical edges of $S(K)$ are four times of those of the edges of K. We assume that all the right-angle sides of $S(K), K \in \mathcal{T}_h$, have the same length denoted by h_S. Recall the definition of the $d = \min_{K \in \mathcal{T}_h} d_K$. Define

$$\tilde{d} = (h_S - h)/3. \tag{6.1}$$

It is clear that $d \eqsim \tilde{d}$. See Figure 2, for an illustration.

In all of these computations, we have used highly resolved numerical solutions obtained using the traditional linear finite element method with mesh size $h_f = 1/4096$ as the reference solutions which are denoted as u_e. Denoting u_h as the numerical solutions computed by the methods considered in this section, we measure the relative error in L^2, L^∞ and energy norms as following:

$$\frac{\|u_h - u_e\|_{L^2}}{\|u_e\|_{L^2}}, \frac{\|u_h - u_e\|_{L^\infty}}{\|u_e\|_{L^\infty}}, \frac{\|u_h - u_e\|_{1,h}}{\|u_e\|_{1,h}},$$

where

$$\|v\|_{1,h} := \left(\sum_{K \in \mathcal{T}_h} \|(\mathbf{a}^\varepsilon)^{1/2} \nabla v\|^2_{L^2(K)} + \|v\|^2_{L^2(\Omega)} \right)^{1/2}.$$

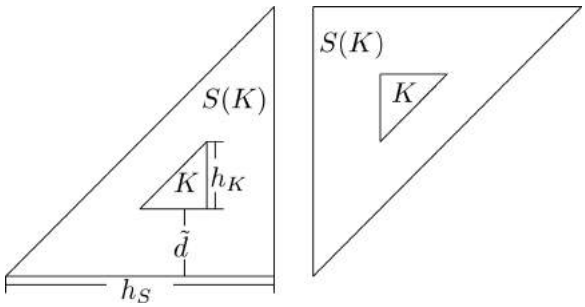

FIGURE 2 The element K and its oversampling element $S(K)$: lower-right elements (left) and upper-left elements (right)

In all tests, the coefficient $\mathbf{a}^\varepsilon$ is chosen as the form $\mathbf{a}^\varepsilon = a^\varepsilon I$, where a^ε is a scalar function and I is the 2 by 2 identity matrix.

6.1 | Application to elliptic problems with highly oscillating coefficients

We first consider the model problem (2.1) in the squared domain $\Omega = [0,1] \times [0,1]$. Assume that $f = 1$ and the coefficient $\mathbf{a}^\varepsilon(x_1, x_2)$ has the following periodic form:

$$\mathbf{a}^\varepsilon(x_1, x_2) = \frac{2 + 1.8\sin(2\pi x_1/\varepsilon)}{2 + 1.8\cos(2\pi x_2/\varepsilon)} + \frac{2 + 1.8\sin(2\pi x_2/\varepsilon)}{2 + 1.8\sin(2\pi x_1/\varepsilon)}, \tag{6.2}$$

where we fix $\varepsilon = 1/100$.

In this test, we choose $h = 1/32$ and report errors in the L^2, L^∞ and energy norms in Table 1. We can see that MsDPGM and MsDGM give more accurate results than the other multiscale methods considered here, while FEM and DGM give worse approximations to the gradient of the solution. We also compare the CPU times T_1 and T_2 spent by MsDGM and MsDPGM, where T_1 is the CPU time of assembling the stiffness matrix, and T_2 is the CPU time of solving the discrete system of algebraic equations. We can observe that the CPU time T_1 of our MsDPGM for assembling the stiffness matrix is shorter than that of MsDGM. For MsDPGM, the main computational cost of assembling the stiffness matrix is to compute the element stiffness matrix which has entries of the type

$$\int_K \mathbf{a}^\varepsilon \nabla\phi_i \cdot \nabla\varphi_j, \qquad \phi_i \in V_{h,dc}^{ms},\ \varphi_j \in V_{h,dc}, \tag{6.3}$$

TABLE 1 Relative errors in the L^2, L^∞, and energy norms for the model problem with periodic coefficient given by (6.2). $\rho = \varepsilon = 1/100, \tilde{d} = h = 1/32, \gamma_0 = 20$.

Relative error	L^2	L^∞	Energy norm	CPU time(s)	
				T_1	T_2
FEM	0.1150 e−00	0.2311 e−00	0.8790 e−00	–	–
DGM	0.2667 e−00	0.2634 e−00	0.5498 e−00	–	–
MsPGM	0.7448 e−01	0.7342 e−01	0.2929 e−00	–	–
OMsPGM	0.1430 e−01	0.1521 e−01	0.1641 e−00	–	–
MsDGM	0.1007 e−01	0.1029 e−01	0.1629 e−00	1.300	0.028
MsDPGM	0.1266 e−01	0.1395 e−01	0.1631 e−00	1.119	0.027

TABLE 2 Relative errors in the L^2, L^∞, and energy norms with respect to the penalty parameter γ_0 for MsDPGM to solve the model problem with periodic coefficient given by (6.2). $\rho = \varepsilon = 1/100, \tilde{d} = h = 1/32$.

Relative error	L^2	L^∞	Energy norm
$\gamma_0 = 10$	0.1100 e−01	0.1266 e−01	0.1637 e−00
$\gamma_0 = 20$	0.1266 e−01	0.1395 e−01	0.1631 e−00
$\gamma_0 = 100$	0.1397 e−01	0.1496 e−01	0.1638 e−00
$\gamma_0 = 1000$	0.1426 e−01	0.1519 e−01	0.1641 e−00
$\gamma_0 = 10000$	0.1429 e−01	0.1521 e−01	0.1641 e−00

where $V_{h,dc}^{ms}$ is the discontinuous multiscale approximation space and $V_{h,dc}$ is the discontinuous linear space. Using the fact that $\nabla\varphi_j, \varphi_j \in V_{h,dc}$ is a constant in element K, we save some CPU time in the computing of integral (6.3).

Second, we do an experiment to study how the penalty parameter γ_0 affects the errors. We fix $\rho = \varepsilon = 1/100, \tilde{d} = h = 1/32$ and choose a series of γ_0 in the test. The results are shown in Table 2. We observe that as γ_0 grows larger, the relative error is close to the error of the OMsPGM. It seems that MsDPGM converges to OMsPGM as the penalty parameter γ_0 grows to infinity (cf. [64]).

The third numerical experiment demonstrates the role of the mesh size h described in Theorem 5.3. We fix $\tilde{d} = 1/32$ and $\varepsilon = 1/100$. Four kinds of mesh size are chosen: $h = 1/64, 1/32, 1/16, 1/8$. The results are given in Table 3. Relative error in energy norm against the mesh size h is depicted in Figure 3. It is easy to see that as h grows larger, the relative error in energy norm grows larger, which is in agreement with the theoretical results in Theorem 5.3. We remark that the classical oversampling MsFEM suffers from the resonance error since the H^1–error estimate has the term ε/h due to the nonconforming error (see [3]). To show the difference, we list the corresponding errors in Table 3 and plot the error in energy norm in Figure 3, respectively. It is easy to see that as h grows larger, the relative error in energy norm of MsFEM grows lower first and higher later, which is in agreement with the fact that its error has the nonconforming error ε/h. However, for MsDPGM, the error estimate in Theorem 5.3, and the numerical results in Table 3 and Figure 3 show that the resonance error has been removed completely.

6.2 | Affection of the size of the oversampling patches

In this subsection, we study how the size of oversampling elements affects the error. The experiment to verify the inequality (4.7) for the model example with coefficient (6.2) has been done in [45]. The figures have been shown that $\|\nabla\eta^j\|_{L^\infty(K)} \cdot d_K$ is bounded by a constant, which is consistent with (4.7); (see Figure 5 in [45]).

TABLE 3 Relative errors in the L^2 and energy norms with respect to the mesh size h for MsDPGM and the oversampling MsFEM to solve the model problem with periodic coefficient given by (6.2). $\rho = \varepsilon = 1/100, \tilde{d} = 1/32, \gamma_0 = 20$.

Relative error	MsDPGM		MsFEM	
	L^2	Energy norm	L^2	Energy norm
$h = 1/64$	0.1371 e−01	0.1593 e−00	0.1200 e−01	0.1771 e−00
$h = 1/32$	0.1266 e−01	0.1631 e−00	0.1676 e−01	0.1644 e−00
$h = 1/16$	0.1948 e−01	0.1870 e−00	0.2438 e−01	0.1902 e−00
$h = 1/8$	0.5210 e−01	0.2620 e−00	0.5659 e−01	0.2682 e−00

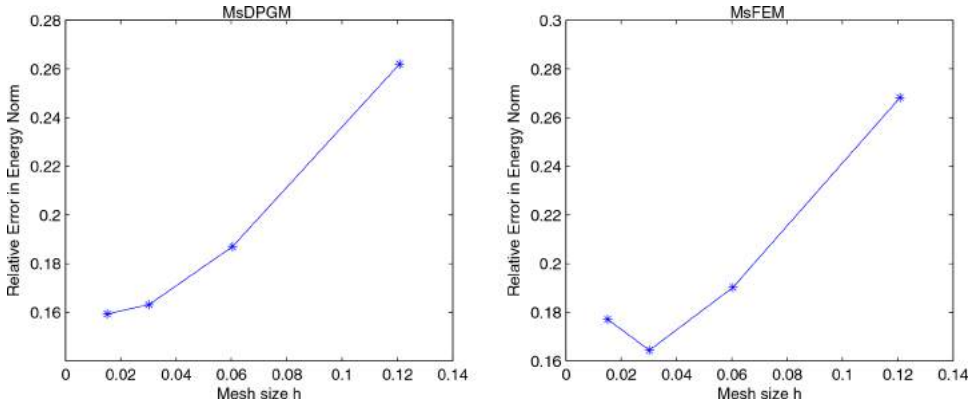

FIGURE 3 Relative error in energy norm against the mesh size h [Color figure can be viewed at wileyonlinelibrary.com]

The following numerical experiment demonstrates the affection of the size of the oversampling patches. Recalling the requirement of the oversampling size $d_K \geq \delta_0 h_K$, we show the relative oversampling size δ_0 against the error. Note the distance $d = \min_{K \in \mathcal{T}_h} d_K$, which is equivalent to $d \geq \delta_0 h$. We set $\rho = \varepsilon = 1/100, h = 1/32$. The result is shown in Table 4. We can see that as δ_0 (equivalently $\tilde{d}$) grows larger, the relative error in energy norm shrinks, which matches the theoretical results in Theorem 5.3. We also notice that when $\tilde{d}$ is close to $\sqrt{\varepsilon}$, the errors begin to decrease very slowly. Recall that there is a homogenization error $\sqrt{\varepsilon}$ in the error estimate (5.6). We think that when d is large enough, $\sqrt{\varepsilon}$ becomes the dominated error instead of ε/d.

6.3 | Application to multiscale problems on L–shape domain

We consider the multiscale problem on the L–shaped domain of Figure 4 with Dirichlet boundary condition so chosen that the true solution is $u = r^{\frac{1}{3}} \sin(2\theta/3)$ in polar coordinates. It is known that the solution has the singular behavior around reentrant corners. So, the classical finite element method fails to provide a satisfactory result.

First, we simulate the problem with coefficient given by (6.2). We fix $\varepsilon = 1/100$ and choose $h = 1/16$. The relative errors are shown in Table 5. We observe that both MsDPGM and MsDGM give better approximation than the other MsPG methods.

TABLE 4 Relative errors in the L^2, L^∞, and energy norms with respect to the relative oversampling size δ_0 for MsDPGM to solve the model problem with periodic coefficient given by (6.2). $\rho = \varepsilon = 1/100, h = 1/32, \gamma_0 = 20$.

Relative error	L^2	L^∞	Energy norm
$\delta_0 = 1/32$	0.4304 e−01	0.4423 e−01	0.2184 e−00
$\delta_0 = 1/16$	0.2924 e−01	0.3172 e−01	0.1893 e−00
$\delta_0 = 1/8$	0.1969 e−01	0.2156 e−01	0.1728 e−00
$\delta_0 = 1/4$	0.1790 e−01	0.2372 e−01	0.1653 e−00
$\delta_0 = 1/2$	0.1531 e−01	0.1766 e−01	0.1642 e−00
$\delta_0 = 1$	0.1266 e−01	0.1295 e−01	0.1631 e−00
$\delta_0 = 2$	0.1197 e−01	0.1398 e−01	0.1631 e−00

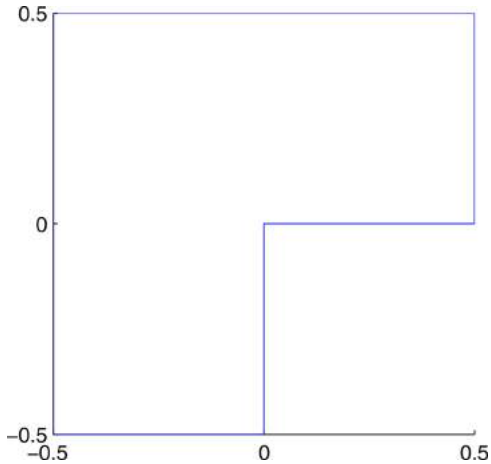

FIGURE 4 The L–shape domain [Color figure can be viewed at wileyonlinelibrary.com]

Second, we simulate the problem with the random log-normal permeability field $\mathbf{a}(x)$, which is generated by using the moving ellipse average [8] with the variance of the logarithm of the permeability $\sigma^2 = 1.0$, and the correlation lengths $l_1 = l_2 = 0.01$ in x_1 and x_2 directions, respectively. One realization of the resulting permeability field is depicted in Figure 5, where $\frac{a_{\max}(x)}{a_{\min}(x)} = 2.9642e + 003$. In this test, we set $\rho = h = 1/16$ since there is no explicit ε in the example. The results are shown in Table 6. We can see that MsDPGM gives a better approximation than the other MsPG methods, while the standard MsPGM gives the wrong approximation to the gradient of solution.

7 | CONCLUSION

In this article, we have proposed a new Petrov–Galerkin method based on the discontinuous multiscale approximation space for multiscale elliptic problems. Under some assumptions regarding the coefficients, we give the error analysis of our method. The H^1–error is of the order

$$O\left(\sqrt{\varepsilon} + \frac{\varepsilon}{d} + h + \frac{h^{3/2}}{\sqrt{\varepsilon}}\right),$$

which consists of the oversampling multiscale approximation error and the error contributed by the penalty. The unpleasant resonance error does not appear as our method uses discontinuous piecewise linear functions as test functions, which are needed only to estimate the interpolation error. Several numerical experiments have demonstrated the efficiency of MsDPGM. We also study the corresponding MsDGM, which couples the classical oversampling multiscale basis with DGM. Our convergence

TABLE 5 Relative errors in the L^2, L^∞, and energy norm for the L–shaped problem with periodic coefficient (6.2). $\rho = \varepsilon = 1/100, \tilde{d} = h = 1/16, \gamma_0 = 20$.

Relative error	L^2	L^∞	Energy norm
MsPGM	0.7765 e−02	0.3635 e−01	0.2014 e−00
OMsPGM	0.6285 e−02	0.3277 e−01	0.1035 e−00
MsDGM	0.3903 e−02	0.2244 e−01	0.9260 e−01
MsDPGM	0.4654 e−02	0.2299 e−01	0.9275 e−01

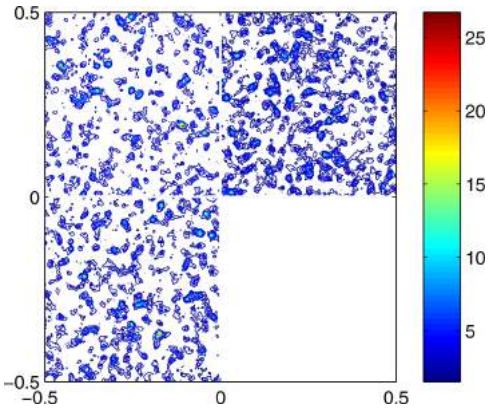

FIGURE 5 The random log-normal permeability field $\mathbf{a}(x)$. $\frac{a_{\max}(x)}{a_{\min}(x)} = 2.9642e+003$ [Color figure can be viewed at wileyonlinelibrary.com]

analysis shows that MsDGM can also eliminate the resonance error completely. That is the reason why MsDGM works just as well, if not slightly better than MsDPGM. Furthermore, we can see that the CPU-time cost of MsDPGM for assembling the stiffness matrix is lower than that of the MsDGM due to its PG version. Therefore, MsDPGM is a good choice considering both the computational accuracy and the computer capacity simultaneously.

We emphasize that the proposed method is not restricted to the periodic case. The numerical experiments show that it is highly applicable to the random coefficient case. However, with the classical oversampling multiscale basis function space introduced in [2], the error estimate method is based on the classical homogenization theory, which needs the assumption that the oscillating coefficient is periodic. In the future, we plan to combine the Petrov–Galerkin method with the new oversampling multiscale space [55] to consider elliptic multiscale problems without any assumption on scale separation or periodicity. Besides, the introduced method may be inefficient for multiscale problems that have singularities, such as the Dirac function singularities, which stem from the simulation of steady flow transport through highly heterogeneous porous media driven by extraction wells [65] or high-conductivity channels that connect the boundaries of coarse-grid blocks [66]. To solve these problems, it needs special definitions of the multiscale basis functions around the channels such as the local spectral basis functions (see [66]) or local refinement of the elements near the channels (see [44]). We will couple these techniques with the introduced method in our future work. Finally, we remark that Generalized Multiscale Finite Element method coupling DGM was explored in [46]. The computation is divided into two stages: offline and online. In the offline stage, they construct a reduced dimensional multiscale space for rapid computations in the online stage. In the online stage, they use the basis functions computed offline to solve the problem for the current realization of the parameters. Similar to MsDPGM, in the online stage, we can use the Petrov–Galerkin version of DGM to solve the

TABLE 6 Relative errors in the L^2, L^∞, and energy norm for the L–shaped problem with random coefficient $\sigma^2 = 1.0$ and $l_1 = l_2 = 0.01$. $\tilde{d} = \rho = h = 1/16, \gamma_0 = 20$.

Relative error	L^2	L^∞	Energy norm
MsPGM	0.9074 e−00	0.1290 e+01	0.6601 e+02
OMsPGM	0.9307 e−02	0.3851 e−01	0.1428 e−00
MsDGM	0.6504 e−02	0.3718 e−01	0.9931 e−01
MsDPGM	0.8587 e−02	0.3810 e−01	0.1013 e−00

problem with the basis functions computed offline, which leads to one kind of Generalized Multiscale Discontinuous Petrov-Galerkin method. The difficulty is the choice of the test function space and the proof of inf-sup condition, which are worth studying.

ACKNOWLEDGMENTS

The authors would like to thank the referees for their carefully reading and constructive comments that helped us improve the paper.

ORCID


Weibing Deng http://orcid.org/0000-0002-6314-1674

REFERENCES

[1] Y. Efendiev, T. Y. Hou, X. H. Wu, *Convergence of a nonconforming multiscale finite element method*, SIAM J. Numer. Anal. 37 (2000) pp. 888–910.

[2] T. Y. Hou, X. H. Wu, *A multiscale finite element method for elliptic problems in composite materials and porous media*, J. Comput. Phys. 134 (1997) pp. 169–189.

[3] T. Y. Hou, X. H. Wu, Z. Cai, *Convergence of a multiscale finite element method for elliptic problems with rapidly oscillation coefficients*, Math. Comp., 68 (1999) pp. 913–943.

[4] W. E, B. Engquist, *The heterogeneous multiscale methods*, Commun. Math. Sci. 1 (2003) pp. 87–132.

[5] W. E, B. Engquist, *Multiscale modeling and computation*, Notice Amer. Math. Soc. 50 (2003) pp. 1062–1070.

[6] W. E, P. Ming, P. Zhang, *Analysis of the heterogeneous multiscale method for elliptic homogenization problems*, J. Am. Math. Soc. 18 (2005) pp. 121–156.

[7] Z. Chen, W. B. Deng, H. Ye, A new upscaling method for the solute transport equations, Discrete and Continuous Dynamical Systems-series A, 13 (2005) pp. 941–960.

[8] L. Durlofsky, *Numerical calculation of equivalent grid block permeability tensors for heterogeneous porous media*, Water Resour Res. 27 (1991) pp. 699–708.

[9] R. E. Ewing, *Aspects of upscaling in simulation of flow in porous media*, Adv. Water Resour. 20 (1997) pp. 349–358.

[10] C. L. Farmer, Upscaling: A review, in Proceedings of the Institute of Computational Fluid Dynamics Conference on Numerical Methods for Fluid Dynamics, Oxford, UK, 2001.

[11] F. Brezzi, L. P. Franca, T. J. R. Hughes, A. Russo, $b = \int g$, Comput. Methods Appl. Mech. Engrg. 145 (1997) pp. 329–339.

[12] F. Brezzi, D. Marini, E. Süli, *Residual-free bubbles for advection-diffusion problems: The general error analysis*, Numer. Math. 85 (2000) pp. 31–47.

[13] T. Hughes, G. R. Feijöo, L. Mazzei, J.-B. Quincy, *The variational multiscale method a paradigm for computational mechanics*, Comput. Meth. Appl. Mech. Eng. 166 (1998) pp. 3–24.

[14] T. Hughes, *Multiscale phenomena: Green's functions, the Dirichlet to Neumann formulation, subgrid scale models, bubbles and the origin of stabilized methods*, Comput. Meth. Appl. Mech. Eng. 127 (1995) pp. 387–401.

[15] G. Sangalli, *Capturing small scales in elliptic problems using a residual-free bubbles finite element method*, Multiscale Model. Simul. 1 (2003) pp. 485–503.

[16] M. Dorobantu, B. Engquist, *Wavelet-based numerical homogenization*, SIAM J. Numer. Anal. 35 (1998) pp. 540–559.

[17] B. Engquist, O. Runborg, Wavelet-based numerical homogenization with applications, in *Multiscale and Multiresolution Methods: Theory and Applications*, T. Barth, T. Chan, and R. Heimes, eds., vol. 20 of Lecture Notes in Computational Sciences and Engineering, Springer-Verlag, Berlin, 2002, pp. 97–148.

[18] J. Fish, V. Belsky, *Multigrid method for a periodic heterogeneous medium, Part II: Multiscale modeling and quality in multidimensional case*, Comput. Meth. Appl. Mech. Eng. 126 (1995) pp. 17–38.

[19] J. D. Moulton, J. E. Dendy, J. M. Hyman, *The black box multigrid numerical homogenization algorithm*, J. Comput. Phys. 141 (1998) pp. 1–29.

[20] J. E. Aarnes, *On the use of a mixed multiscale finite element method for greater flexibility and increased speed or improved accuracy in reservoir simulation*, Multiscale Model. Simul. 2 (2004) pp. 421–439.

[21] J. E. Aarnes, Y. Efendiev, *Mixed multiscale finite element methods for stochastic porous media flows*, SIAM J. Sci. Comput. 30 (2008) pp. 2319–2339.

[22] J. E. Aarnes, Y. Efendiev, L. Jiang, *Mixed multiscale finite element methods using limited global information*, Multiscale Model. Simul. 7 (2008) pp. 655–676.

[23] Z. Chen, T. Y. Hou, *A mixed multiscale finite method for elliptic problems with oscillating coefficients*, Math. Comp. 72 (2002) pp. 541–576.

[24] Z. X. Chen, *Multiscale methods for elliptic homogenization problems*, Numer. Methods Partial Differential Eq. 22 (2006) pp. 317–360.

[25] Z. X. Chen, M. Cui, T. Y. Savchuk, X. Yu, *The multiscale finite element method with nonconforming elements for elliptic homogenization problems*, Multiscale Model. Simul. 7 (2008) pp. 517–538.

[26] Z. X. Chen, T. Y. Savchuk, *Analysis of the multiscale finite element method for nonlinear and random homogenization problems*, SIAM J. Numer. Anal. 46 (2007/08) pp. 260–279.

[27] W. Deng, X. Yun, C. Xie, *Convergence analysis of the multiscale method for a class of convection-diffusion equations with highly oscillating coefficients*, Appl. Numer. Math. 59 (2009) pp. 1549–1567.

[28] Y. Efendiev, V. Ginting, T. Y. Hou, R. Ewing, *Accurate multiscale finite element methods for two-phase flow simulations*, J. Comput. Phys. 220 (2006) pp. 155–174.

[29] Y. Efendiev, T. Hou, *Multiscale finite element methods for porous media flows and their applications*, Appl. Numer. Math. 57 (2007) pp. 577–596.

[30] T. Y. Hou, X. H. Wu, Y. Zhang, *Removing the cell resonance error in the multiscale finite element method via a Petrov-Galerkin formulation*, Commun. Math. Sci. 2 (2004) pp. 185–205.

[31] P. Jenny, S. Lee, H. Tchelepi, *Multi-scale finite-volume method for elliptic problems in subsurface flow simulation*, J. Comput. Phys. 187 (2003) pp. 47–67.

[32] Y. Efendiev, T. Y. Hou, *Multiscale finite element methods theory and applications*, Springer, Lexington, KY, 2009.

[33] J. Douglas Jr, T. Dupont, *Interior penalty procedures for elliptic and parabolic Galerkin methods*, Lecture Notes in Phys. 58, Springer-Verlag, Berlin, 1976.

[34] D. Arnold, *An interior penalty finite element method with discontinuous elements*, SIAM J. Numer. Anal. 19 (1982) pp. 742–760.

[35] D. Arnold, F. Brezzi, B. Cockburn, D. Marini, *Unified analysis of discontinuous Galerkin methods for elliptic problems*, SIAM J. Numer. Anal. 39 (2001) pp. 1749–1779.

[36] J. E. Aarnes, B.-O. Heimsund, Multiscale discontinuous Galerkin methods for elliptic problems with multiple scales, Multiscale methods in science and engineering, Lect. Notes Comput. Sci. Eng. Springer, Berlin, 2005, pp. 1–20.

[37] P. Castillo, *A review of the local discontinuous Galerkin (LDG) method applied to elliptic problems*, Appl. Numer. Math. 56 (2006) pp. 1307–1313.

[38] P. Castillo, B. Cockburn, I. Perugia, D. Schötzau, *An a priori error analysis of the local discontinuous Galerkin method for elliptic problems*, SIAM J. Numer. Anal. 38 (2000) pp. 1676–1706.

[39] I. Babuška, *The finite element method with penalty*, Math. Comp. 27 (1973) pp. 221–228.

[40] I. Babuška, M. Zlámal, *Nonconforming elements in the finite element method with penalty*, SIAM J. Numer. Anal. 10 (1973) pp. 863–875.

[41] P. Bastian, C. Engwer, *An unfitted finite element method using discontinuous Galerkin*, Int. J. Numer. Meth. Engng. 79 (2009) pp. 1557–1576.

[42] F. Brezzi, G. Manzini, D. Marini, P. Pietra, A. Russo, *Discontinuous Galerkin approximations for elliptic problems*, Numer. Methods Partial Differential Eq, 16 (2000) pp. 365–378.

[43] Z. X. Chen, H. Chen, *Pointwise error estimates of discontinuous Galerkin methods with penalty for second-order elliptic problems*, SIAM J. Numer. Anal. 42 (2004) pp. 1146–1166.

[44] W. Deng, H. Wu, *A combined finite element and multiscale finite element method for the multiscale elliptic problems*, Multiscale Model. Simul. 12 (2014) pp. 1424–1457.

[45] F. Song, W. Deng, H. Wu, *A combined finite element and oversampling Petrov-Galerkin method for the multiscale elliptic problems with singularities*, J. Comput. Phys. 305 (2016) pp. 722–743.

[46] Y. Efendiev, J. Galvis, R. Lazarov, M. Moon, *Generalized multiscale finite element method, symmetric interior penalty coupling*, J. Comput. Phys. 255 (2013) pp. 1–15.

[47] W. Wang, J. Guzmán, C.-W. Shu, *The multiscale discontinuous Galerkin method for solving a class of second order elliptic problems with rough coefficients*, Int. J. Numer. Anal. Model. 8 (2011) pp. 28–47.

[48] L. Yuan, C.-W. Shu, *Discontinuous Galerkin method for a class of elliptic multi-scale problems*, Internat. J. Numer. Methods Fluids 56 (2008) pp. 1017–1032.

[49] Y. Zhang, W. Wang, J. Guzmán, C.-W. Shu, *multi-scale discontinuous Galerkin method for solving elliptic problems with curvilinear unidirectional rough coefficients*, J. Sci. Comput. 61 (2014) pp. 42–60.

[50] D. Elfverson, E. H. Georgoulis, A. Målqvist, *An adaptive discontinuous Galerkin multiscale method for elliptic problems*, Multiscale Model. Simul. 11 (2013) pp. 747–765.

[51] D. Elfverson, E. H. Georgoulis, A. Målqvist, D. Peterseim, *Convergence of a discontinuous Galerkin multiscale method*, SIAM J. Numer. Anal. 51 (2013) pp. 3351–3372.

[52] A. Abdulle, *Multiscale method based on discontinuous Galerkin methods for homogenization problems*, C. R. Math. Acad. Sci. Paris 346 (2008) pp. 97–102.

[53] A. Abdulle, M. E. Huber, *Discontinuous Galerkin finite element heterogeneous multiscale method for advection-diffusion problems with multiple scales*, Numer. Math. 126 (2014) pp. 589–633.

[54] A. Målqvist and D. Peterseim, *Localization of elliptic multiscale problems*, Math. Comp. 83 (2014) pp. 2583–2603.

[55] P. Henning, D. Peterseim, *Oversampling for the multiscale finite element method*, Multiscale Model. Simul. 11 (2013) pp. 1149–1175.

[56] Z. Chen, H. Wu, *Selected topics in finite element method*, Science Press, Beijing, 2010.

[57] S. Chou, *Analysis and convergence of a covolume method for the generalized stokes problem*, Math. Comput. 66 (1997) pp. 85–104.

[58] K. W. Morton, *Petrov-Galerkin methods for non-self-adjoint problems*, Springer Berlin Heidelberg, 1980.

[59] Y. Epshteyn, B. Riviere, *Estimation of penalty parameters for symmetric interior penalty Galerkin methods*, J. Comput. Appl. Math. 206 (2007) pp. 843–872.

[60] A. Bensoussan, J. L. Lions, G. Papanicolaou, *Asymptotic Analysis for Periodic Structure*, vol. 5 of Studies in Mathematics and Its Application, North-Holland Publ. 1978.

[61] V. V. Jikov, S. M. Kozlov, O. A. Oleinik, *Homogenization of differential operators and integral functionals*, Springer-Verlag, Berlin, 1994.

[62] S. C. Brenner, L. R. Scott, *The mathematical theory of finite element methods*, Springer-Verlag, New York, 2002.

[63] P. G. Ciarlet, *The finite element method for elliptic problems*, North Holland, Amsterdam, 1978.

[64] M. G. Larson, A. J. Niklasson, Conservation properties for the continuous and discontinuous Galerkin methods, Tech. Rep. 2000-08, Chalmers University of Technology, Göteborg, Sweden 2001.

[65] Z. Chen, X. Y. Yue, *Numerical homogenization of well singularities in the flow transport through heterogeneous porous media*, Multiscale Model. Simul. 1 (2003) pp. 260–303.

[66] Y. Efendiev, J. Galvis, X. H. Wu, *Multiscale finite element methods for high-contrast problems using local spectral basis functions*, J. Comput. Phys. 230 (2011) pp. 937–955.

[67] P. Grisvard, *Elliptic problems on nonsmooth domains*, Pitman, Boston, 1985.

[68] F. Song, Analysis and calculation of discontinuous and combined multiscale finite element methods, Ph.D. Thesis, Nanjing University, 2016.

How to cite this article: Song F, Deng W. Multiscale discontinuous Petrov–Galerkin method for the multiscale elliptic problems. *Numer Methods Partial Differential Eq*. 2018;34:184–210. https://doi.org/10.1002/num.22191

APPENDIX A: PROOF OF THEOREM 4.1

The following theorem plays a major role in our analysis (cf. [23, 56]).

Theorem A.1 *Assume that* $u_0 \in H^2(\Omega) \cap W^{1,\infty}(\Omega)$. *There exists a constant* C *independent of* u_0, ε, Ω *such that*

$$\|u_\varepsilon - u_1 - \varepsilon\theta_\varepsilon\|_{H^1(\Omega)} \le C\varepsilon|u_0|_{H^2(\Omega)},$$
$$\|\varepsilon\theta_\varepsilon\|_{H^1(\Omega)} \le C\sqrt{\varepsilon}|u_0|_{W^{1,\infty}(\Omega)} + C\varepsilon|u_0|_{H^2(\Omega)},$$

where θ_ε *denote the boundary corrector defined by*

$$\begin{aligned} -\nabla\cdot(\mathbf{a}^\varepsilon\nabla\theta_\varepsilon) &= 0 && \text{in } \Omega,\\ \theta_\varepsilon &= -\chi^j(x/\varepsilon)\frac{\partial u_0(x)}{\partial x_j} && \text{on } \partial\Omega. \end{aligned} \tag{A.1}$$

We first estimate $|\varepsilon\theta_\varepsilon|_{H^2(\Omega)}$.

Lemma A.1 *Assume that* $u_0 \in H^2(\Omega) \cap W^{1,\infty}(\Omega)$. *Then the following estimate holds:*

$$|\varepsilon\theta_\varepsilon|_{H^2(\Omega)} \lesssim \frac{1}{\sqrt{\varepsilon}}|u_0|_{W^{1,\infty}(\Omega)} + |u_0|_{H^2(\Omega)}. \tag{A.2}$$

Proof We only consider the case where $n=2$. For $n=3$, the proof is similar. Let $\xi \in C_0^\infty(\mathbf{R}^2)$ be the cut-off function such that $0 \le \xi \le 1, \xi = 1$ in $\Omega \setminus \Omega_{\varepsilon/2}, \xi = 0$ in Ω_ε, and $|\nabla\xi| \le C/\varepsilon, |\nabla^2\xi| \le C/\varepsilon^2$ in Ω, where $\Omega_\varepsilon := \{x : \operatorname{dist}\{x, \partial\Omega\} \ge \varepsilon\}$. Then

$$v = \theta_\varepsilon + \xi\left(\chi^j\frac{\partial u_0}{\partial x_j}\right) \in H_0^1(\Omega)$$

satisfies

$$-\nabla\cdot(\mathbf{a}^\varepsilon\nabla v) = -\nabla\cdot\left(\mathbf{a}^\varepsilon\nabla\left(\xi\chi^j\frac{\partial u_0}{\partial x_j}\right)\right) \quad \text{in } \Omega, \qquad v|_{\partial\Omega} = 0. \tag{A.3}$$

By use of Theorem 4.3.1.4 in [67], and together with Theorem A.1, we have

$$\begin{aligned}|v|_{H^2(\Omega)} &\lesssim \frac{1}{\varepsilon}\|v\|_{L^2(\Omega)} + \|\nabla\cdot\left(\mathbf{a}^\varepsilon\nabla\left(\xi\chi^j\frac{\partial u_0}{\partial x_j}\right)\right)\|_{L^2(\Omega)}\\ &\lesssim \frac{\sqrt{\varepsilon}}{\varepsilon^2}|u_0|_{W^{1,\infty}(\Omega)} + \frac{1}{\varepsilon}|u_0|_{H^2(\Omega)},\end{aligned}$$

which implies

$$|\theta_\varepsilon|_{H^2(\Omega)} \lesssim \frac{\sqrt{\varepsilon}}{\varepsilon^2}|u_0|_{W^{1,\infty}(\Omega)} + \frac{1}{\varepsilon}|u_0|_{H^2(\Omega)}. \tag{A.4}$$

This completes the proof. ∎

Proof of Theorem 4.1 It is shown that, for any $\varphi \in H_0^1(\Omega)$ (see [23, p.550] or [56, p.125]),

$$\begin{aligned}&(\mathbf{a}(x/\varepsilon)\nabla(u_\varepsilon - u_1), \nabla\varphi)_\Omega\\ &= (\mathbf{a}^*\nabla u_0, \nabla\varphi)_\Omega - \left(\mathbf{a}(x/\varepsilon)\nabla\left(u_0 + \varepsilon\chi^k\frac{\partial u_0}{\partial x_k}\right), \nabla\varphi\right)_\Omega\\ &= \varepsilon\int_\Omega a_{ij}(x/\varepsilon)\chi^k\frac{\partial^2 u_0}{\partial x_j\partial x_k}\frac{\partial\varphi}{\partial x_i}\mathrm{d}x - \varepsilon\int_\Omega \alpha_{ij}^k(x/\varepsilon)\frac{\partial^2 u_0}{\partial x_j\partial x_k}\frac{\partial\varphi}{\partial x_i}\mathrm{d}x,\end{aligned} \tag{A.5}$$

where $\alpha^k(x/\varepsilon) = (\alpha_{ij}^k(x/\varepsilon))$ are skew-symmetric matrices which satisfy that (see [61, p. 6])

$$G_i^k(y) = \frac{\partial}{\partial y_j}(\alpha_{ij}^k(y)), \qquad \int_Y \alpha_{ij}^k(y)\mathrm{d}y = 0$$

with

$$G_i^k = a_{ik}^* - a_{ij}\left(\delta_{kj} + \frac{\partial\chi^k}{\partial y_j}\right).$$

From (A.5), it follows that,

$$\nabla\cdot(\mathbf{a}(x/\varepsilon)\nabla(u_\varepsilon - u_1)) = \varepsilon\frac{\partial}{\partial x_i}\left(a_{ij}(x/\varepsilon)\chi^k\frac{\partial^2 u_0}{\partial x_j\partial x_k} - \alpha_{ij}^k(x/\varepsilon)\frac{\partial^2 u_0}{\partial x_j\partial x_k}\right),$$

which combing the definition of θ_ε, yields

$$\nabla\cdot(\mathbf{a}(x/\varepsilon)\nabla(u_\varepsilon - u_1 - \varepsilon\theta_\varepsilon)) = \varepsilon\frac{\partial}{\partial x_i}\left(a_{ij}(x/\varepsilon)\chi^k\frac{\partial^2 u_0}{\partial x_j\partial x_k} - \alpha_{ij}^k(x/\varepsilon)\frac{\partial^2 u_0}{\partial x_j\partial x_k}\right).$$

Thus, from Theorem 4.3.1.4 in [67], it follows that

$$|u_\varepsilon - u_1 - \varepsilon\theta_\varepsilon|_{H^2(\Omega)} \lesssim \frac{1}{\varepsilon}\|u_\varepsilon - u_1\|_{L^2(\Omega)} + |u_0|_{H^2(\Omega)} + \varepsilon|u_0|_{H^3(\Omega)}, \tag{A.6}$$

which combing (A.2) and Theorem A.1, yields (4.2) immediately. ∎

APPENDIX B: THEORETICAL RESULTS OF MSDGM

We give some theoretical results of MsDGM here for the convenience of the reader. Detailed analysis can be found in the first author's Ph.D. thesis [68].

Lemma B.1 *We have*

$$|a(\tilde{u}_h, v_h)| \leq C\|\tilde{u}_h\|_E\|v_h\|_E \qquad \forall \tilde{u}_h, v_h \in V_{h,dc}^{ms}. \tag{B.1}$$

Further, let the assumptions of Lemma 4.4 be fulfilled and γ_0 is large enough, then

$$a(v_h, v_h) \geq \frac{1}{2}\|v_h\|_E^2 \qquad \forall v_h \in V_{h,dc}^{ms}. \tag{B.2}$$

Here

$$\|v\|_E := \left(\sum_{K\in\mathcal{T}_h}\int_K \mathbf{a}^\varepsilon|\nabla v|^2\mathrm{d}x + \sum_{e\in\Gamma_h\cup\partial\Omega}\frac{\rho}{\gamma_0}\int_e\{\mathbf{a}^\varepsilon\nabla v\cdot\mathbf{n}\}^2\mathrm{d}s + \sum_{e\in\Gamma_h\cup\partial\Omega}\frac{\gamma_0}{\rho}\int_e[v]^2\mathrm{d}s\right)^{1/2} \qquad \forall v \in V_{h,dc}^{ms}.$$

Using the definition of the above norm, the Cauchy-Schwarz inequality and (4.8), Lemma 4.4, we can obtain (B.1) and (B.2) immediately. The proof is similar to Theorem 5.1 and is omitted here.

Theorem B.1 *Let u_ε be the solution of (2.1), and let $\tilde{u}_h$ be the numerical solution computed by MsDGM defined in (3.4). Assume that $u_0 \in H^3(\Omega), f \in L^2(\Omega)$, $\varepsilon \lesssim h \lesssim d$, and that the penalty parameter γ_0 is large enough. Then there exists a constant γ independent of h and ε such that if $\varepsilon/h_K \leq \gamma$ for all $K \in \mathcal{T}_h$, the following error estimate holds:*

$$\|u_\varepsilon - \tilde{u}_h\|_E \lesssim h + \frac{h^{3/2}}{\sqrt{\varepsilon}} + \sqrt{\varepsilon} + \frac{\varepsilon}{d}, \tag{B.3}$$

where $d = min_{K\in\mathcal{T}_h} d_K$.

Proof By use of the Galerkin orthogonality of $a(\cdot,\cdot)$, we only need to estimate the interpolation error.

Take v_h as ψ_h (see (5.7)). The following two estimates of the error have been shown in the proof of Theorem 5.3:

$$\left(\sum_{K\in\mathcal{T}_h}\|(\mathbf{a}^\varepsilon)^{1/2}\nabla(u_\varepsilon - v_h)\|_{L^2(K)}^2\right)^{\frac{1}{2}} \lesssim h|u_0|_{H^2(\Omega)} + \left(\sqrt{\varepsilon} + \frac{\varepsilon}{d}\right)|u_0|_{W^{1,\infty}(\Omega)}, \tag{B.4}$$

and

$$\sum_{e\in\Gamma_h\cup\partial\Omega}\frac{\varepsilon}{\gamma_0}\|\{\mathbf{a}^\varepsilon\nabla(u_\varepsilon-v_h)\cdot\mathbf{n}\}\|^2_{L^2(e)}\lesssim h^2|u_0|^2_{H^2(\Omega)}+\varepsilon|u_0|^2_{W^{1,\infty}(\Omega)}+\varepsilon^4|u_0|^2_{H^3(\Omega)}. \tag{B.5}$$

It remains to consider the term $\sum_{e\in\Gamma_h\cup\partial\Omega}\frac{\gamma_0}{\varepsilon}\|[u_\varepsilon-v_h]\|^2_{L^2(e)}$. Noting that $[u_\varepsilon]=[u_1]=0$, then by use of the trace inequality (4.8) and Lemma 4.2, we have

$$\begin{aligned}\sum_{e\in\Gamma_h\cup\partial\Omega}\frac{\gamma_0}{\varepsilon}\|[u_\varepsilon-v_h]\|^2_{L^2(e)}&\lesssim\sum_{e\in\Gamma_h\cup\partial\Omega}\frac{\gamma_0}{\varepsilon}\|[u_1-v_h]\|^2_{L^2(e)}\\&\lesssim\varepsilon^{-1}h^{-1}\sum_{K\in\mathcal{T}_h}\|u_1-v_h\|^2_{L^2(K)}\\&\quad+\varepsilon^{-1}\left(\sum_{K\in\mathcal{T}_h}\|u_1-v_h\|^2_{L^2(K)}\right)^{1/2}\left(\sum_{K\in\mathcal{T}_h}\|\nabla(u_1-v_h)\|^2_{L^2(K)}\right)^{1/2}\\&\lesssim\frac{h^3}{\varepsilon}|u_0|^2_{H^2(\Omega)}+\varepsilon|u_0|^2_{W^{1,\infty}(\Omega)},\end{aligned} \tag{B.6}$$

where we have used the assumption $\varepsilon\lesssim h\lesssim d$ and the Young's inequality to derive the above inequality.

Hence, from (B.4), (B.5), and (B.6), it follows (B.3) immediately. This completes the proof. ∎